



PHYSICAL SCIENCES

Magnon-lattice propagation in a Morse chain: the role played by the spin-lattice interaction and the initial condition

MARCONI SILVA SANTOS JUNIOR, MESSIAS DE OLIVEIRA SALES &
FRANCISCO ANACLETO BARROS FIDELIS DE MOURA

Abstract: Our research focuses on studying magnon dynamics in a Morse lattice. We used a Heisenberg Hamiltonian to represent the spins while a Morse formalism governed the lattice deformations. The strength of the spin-spin interaction depended on the distance between neighboring spins, which followed an exponential pattern. We explored various initial conditions for the lattice and spin wave function and observed how they affected the magnon-lattice propagation. Additionally, we analyzed the impact of the parameter that controlled the difference in time scales between spin and lattice deformation propagation.

Key words: localization, disorder, Anderson localization, nonlinear lattice.

INTRODUCTION

The magnon dynamics under the effect of magnetoelastic coupling has attracted a high interest Masciocchi et al. (2022), Chen et al. (2023), Luo et al. (2023), Gries et al. (2022), Cong et al. (2022), Challali et al. (2023), Sun et al. (2022), Holanda et al. (2018), Xiong et al. (2017), Li et al. (2020), Hayashi & Ando (2018), Weiler et al. (2012), Zhang et al. (2019, 2020), Sasaki et al. (2021), Mingran et al. (2020), Morais et al. (2021), Sales et al. (2018, 2023). In Chen et al. (2023), the authors investigate the magnon propagation using a Boltzmann method framework which includes magnon-phonon interaction and diverse scattering terms. They solved the effective equations and detailed some abnormal phenomena observed in several experiments. Zhang et al. (2019) demonstrates that the magnon-phonon coupling controls the thermal Hall effect on a ferromagnetic square lattice featuring Dzyaloshinskii-Moriya interaction. Li et al. (2020) reported the existence of collective antiferromagnetic magnon-phonon pair formation in an insulator Cr_2O_3 . The results in ref. Hayashi & Ando (2018) indicate that the magnon-phonon coupling could amplify spin pumping in a Pt/YIG bi-layer film. Mingran et al. (2020) reported the first observation of the magneto-rotation coupling in a perpendicularly anisotropic magnetic film. They also introduce the theoretical background. Sales et al. (2018) investigated the magnon propagation in a Fermi-Pasta-Ulam. They studied the spin dynamics using a quantum Heisenberg Hamiltonian with the ferromagnetic ground state. The magnon-lattice interaction was introduced by considering the spin-spin interaction terms as a function of the distance between the spins. Solving the dynamics equations, they demonstrated the existence of a magnon-soliton mode.

Morais et al. (2021) investigate the propagation of magnon states coupled to the harmonic modes of a linear lattice. It was considered an adiabatic approximation to deduce an effective quantum equation to describe the magnon dynamics. The authors demonstrate the existence of a self-trapping transition to the magnon state. Sales et al. (2018), the dynamics of magnon-lattice it was considered by writing the Heisenberg Hamiltonian in a nonlinear Morse chain. The authors demonstrate that the lattice deformation embodies a finite fraction of the spin wave function in the robust spin-lattice coupling regime, generating a mobile magnon-lattice excitation.

In this work, we revisit the problem of magnon dynamics in a Morse lattice. We designed the spin-spin coupling using a Heisenberg model. The intensity of the spin-spin interaction fits an exponential dependent on the distance between nearest-neighbor spins. This framework provides an effective spin-lattice interaction, and a single tunable parameter controls the intensity of this interaction. We will investigate the magnon-lattice dynamics considering a wide range of initial conditions. Our calculations indicate that the magnon-lattice pair formation strongly depends on the initial condition's width. We will also investigate the dependence of the magnon-lattice propagations as a function of the time-scales difference between spin and lattice propagation. Our results suggest that magnon-lattice pair formation occurs for a small amount of magnon-lattice interaction as the time scale difference increases.

MODEL

Our model is a quantum one-dimensional Heisenberg model with N spin $1/2$ on a nonlinear Morse chain. The spin-spin interaction is strongly dependent on the distance between nearest-neighbor spins. The complete quantum Hamiltonian is given by Evangelou & Katsanos (1992), de Moura et al. (2002):

$$H_S = - \sum_{y=1}^N \{J_{y,y+1} \vec{S}_y \vec{S}_{y+1}\}. \quad (1)$$

The interaction between spins y and $y + 1$ is given by $J_{y,y+1} = J e^{-\alpha(X_{y+1}-X_y)}$. X_y is the displacement of spin y from its equilibrium position. We emphasize again that we are dealing with a one-dimensional geometry. Therefore, without lattice vibrations, all spins are in equally spaced positions (in equilibrium, the distance between nearest-neighbor spins is the lattice spacing, an adimensional parameter $l_s = 1$). However, our model will consider that the spins can move around their equilibrium position. The spatial movement of the spins produces variations in the value of the spin-spin interaction. Our model will consider that these variations follow this exponential dependence shown earlier. The parameter α characterizes this exponential dependence within this formalism, thus controlling the effective spin-lattice interaction. The lattice dynamics here will be governed by a Morse potential represented by the classical Hamiltonian Hennig et al. (2007), Ikeda et al. (2007), de Lima & de Cavalho (2012), Carrillo et al. (2013):

$$H_L = \sum_{y=1}^N \frac{p_y^2}{2} + \sum_{y=1}^N \{1 - \exp[-(X_y - X_{y-1})]\}^2. \quad (2)$$

Here, P_y represents the particle moment at site y . We emphasize that we are using the dimensionless representation considered in ref. Hennig et al. (2007). The time is scaled as $t \rightarrow \omega t$, with ω representing the frequency of oscillations around the minimum of the Morse potential. The energy scale is measured in units of the depth of the Morse potential Hennig et al. (2007). The magnon dynamics is represented by the time-dependent Schrödinger equation for ($\hbar = 1$) defined as Sales et al. (2018):

$$\begin{aligned}
 i \frac{du_y(t)}{dt} = & \frac{\tau}{2} \{ [\exp(-\alpha(X_{y+1} - X_y)) \\
 & + \exp(-\alpha(X_y - X_{y-1}))] u_y(t) \\
 & - \exp(-\alpha(X_y - X_{y-1})) u_{y-1}(t) \\
 & - \exp(-\alpha(X_{y+1} - X_y)) u_{y+1}(t) \}.
 \end{aligned}
 \tag{3}$$

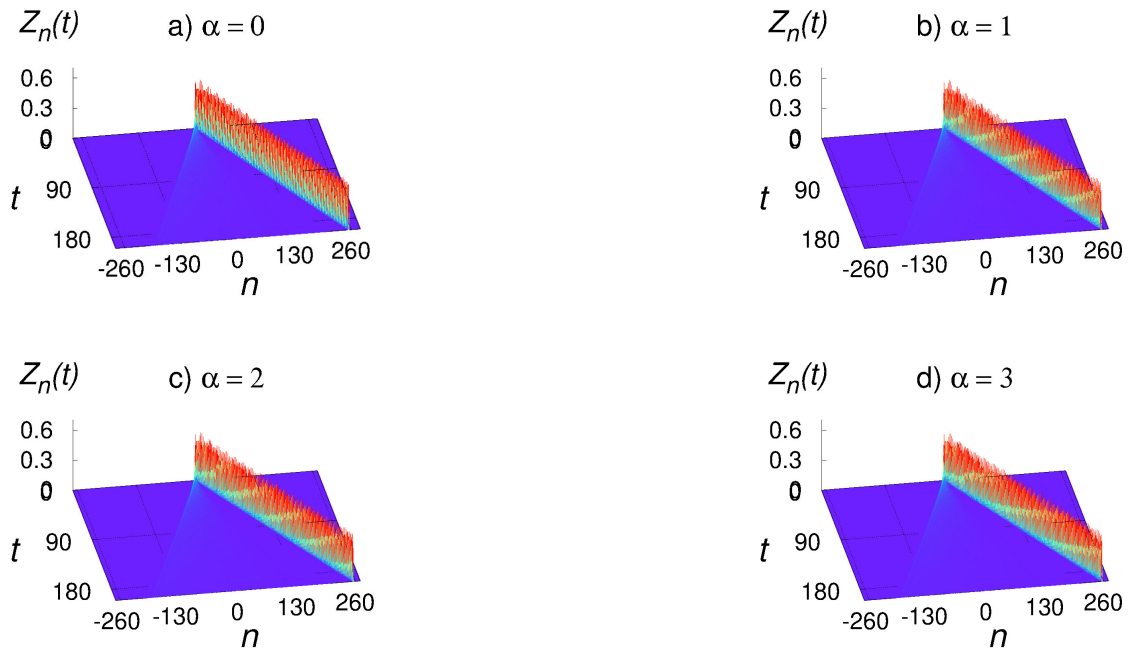


Figure 1. The lattice deformation Z_n versus t and n where $n = y - N/2 = 0$ represents the center of the chain. Calculations were done for $v_0 = 1, \sigma_s = 0.5, \sigma_L = 0.5, \tau = 10$ and $\alpha = 0, 1, 2, 3$

To clarify, we want to point out that the previous equations were written considering a ferromagnetic ground state denoted as $|0\rangle$ and a set of kets represented by $|y\rangle = S_y^+ |0\rangle$. Therefore, the $u_y(t)$ value corresponds to the wave function amplitude associated with the spin deviation at position

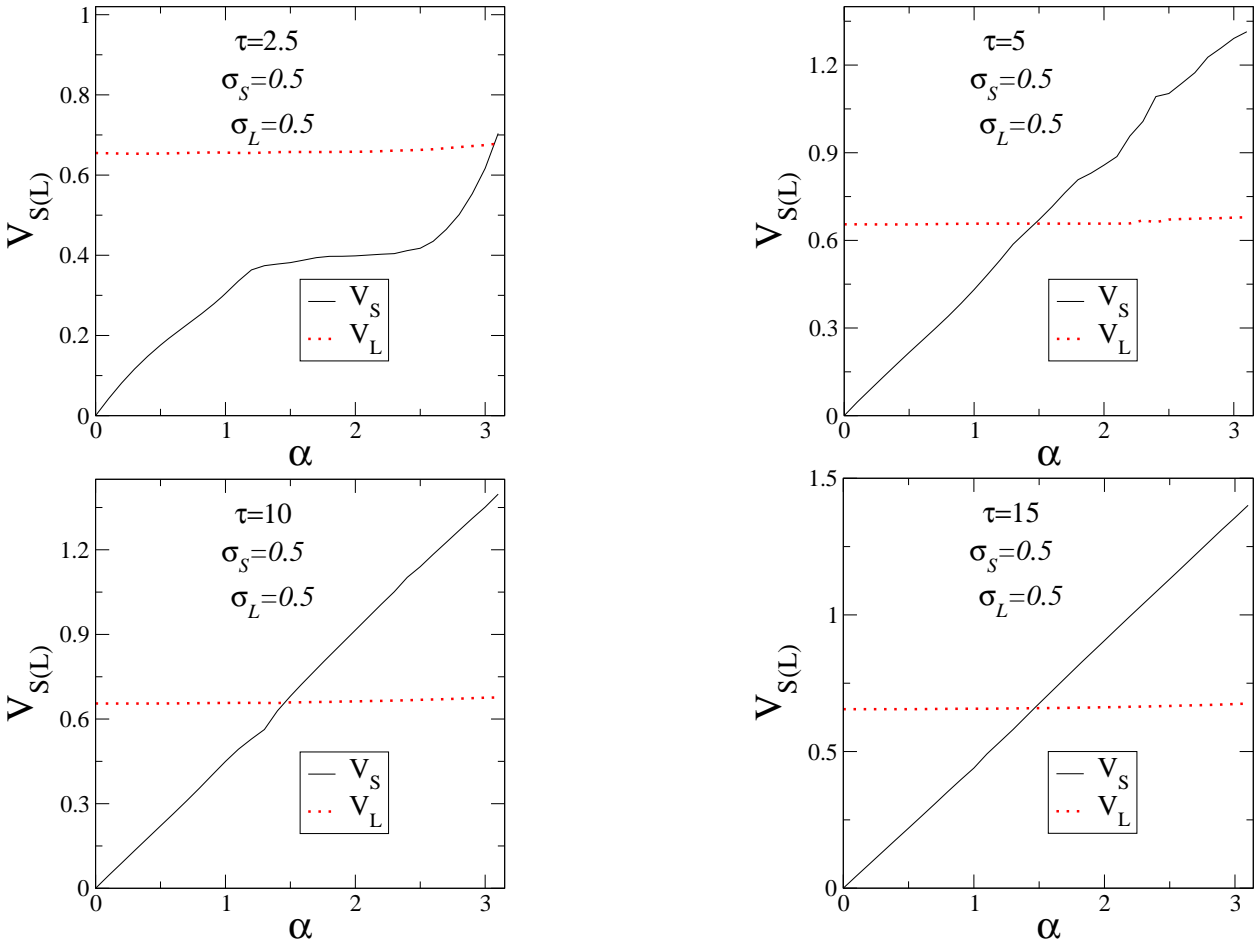


Figure 2. Magnon and lattice deformation velocities [V_S (black solid line) and V_L (red dotted line)] versus α . We have considered $v_0 = 1$, $\sigma_s = 0.5$, $\sigma_l = 0.5$ and $\tau = 2.5$ up to 15.

y. By utilizing the Hamilton formalism, we have derived the equations governing the dynamics of the lattice:

$$\begin{aligned}
 \frac{d^2 X_y}{dt^2} &= \{1 - \exp[-(X_{y+1} - X_y)]\} \exp[-(X_{y+1} - X_y)] \\
 &- \{1 - \exp[-(X_y - X_{y-1})]\} \exp[-(X_y - X_{y-1})] \\
 &+ \frac{J\alpha}{2} \left[e^{-\alpha(X_y - X_{y-1})} (u_y^* u_y + u_{y-1}^* u_{y-1}) \right. \\
 &- e^{-\alpha(X_{y+1} - X_y)} (u_y^* u_y + u_{y+1}^* u_{y+1}) \\
 &+ e^{-\alpha(X_{y+1} - X_y)} (u_{y+1}^* u_y + u_y^* u_{y+1}) \\
 &\left. - e^{-\alpha(X_y - X_{y-1})} (u_{y-1}^* u_y + u_y^* u_{y-1}) \right]. \tag{4}
 \end{aligned}$$

It's important to note that we changed the time scale in the previous equation by rescaling t to ωt , with ω representing the frequency of oscillations around the minimum of the Morse potential Hennig et al. (2007). This step is necessary to account for the difference in timescale between electron dynamics

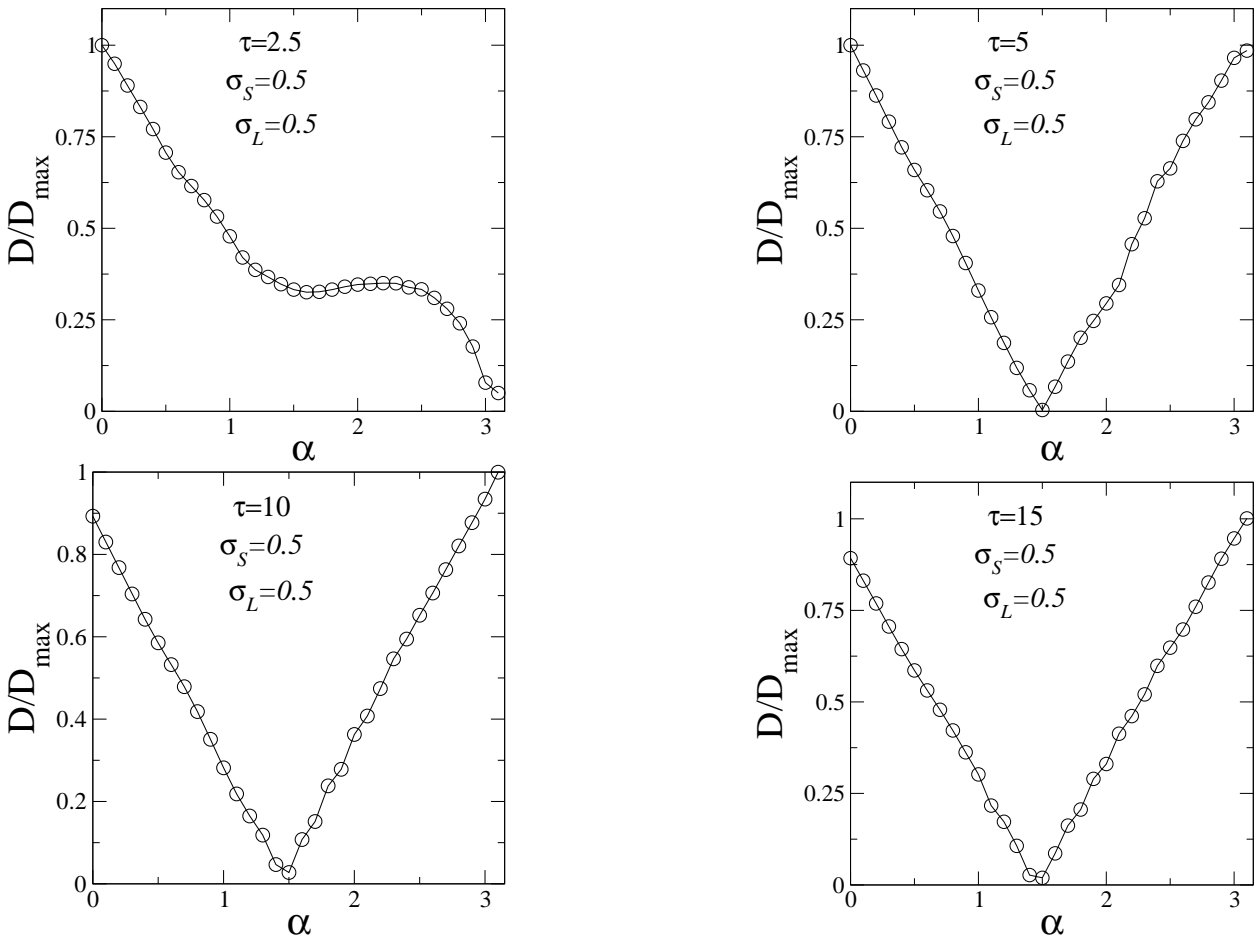


Figure 3. The normalized distance between the Magnon and the lattice deformation (D/D_{max}) versus α . Calculations done for $v_0 = 1$, $\sigma_s = 0.5$, $\sigma_L = 0.5$ and $\tau = 2.5$ up to 15.

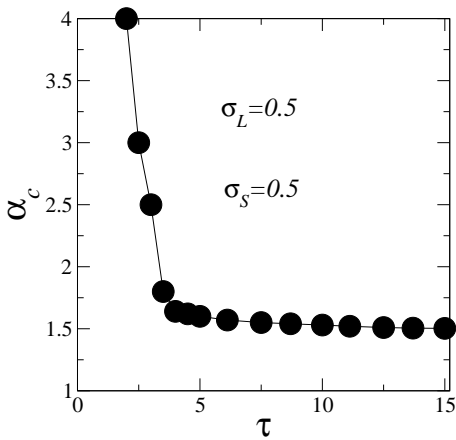


Figure 4. The critical value α_c versus τ for $\sigma_s = \sigma_L = 0.5$.

(which is faster) and lattice vibrations (which is slower) Hennig et al. (2007), Davydov (1991), Scott (1992). To put it simply, this framework involves a factor $\tau = J/(\hbar\omega)$ that multiplies the spin equation Hennig

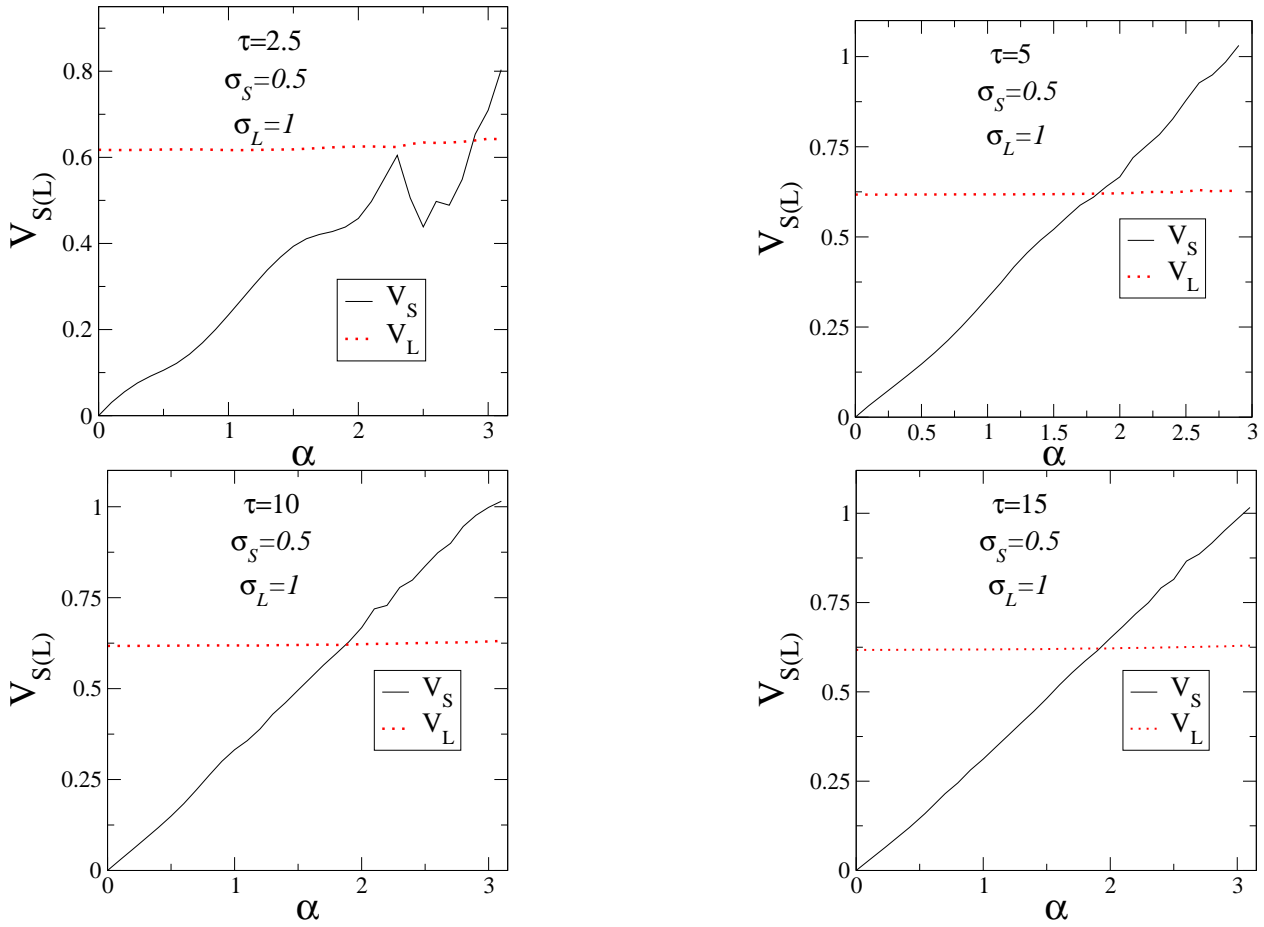


Figure 5. Magnon and lattice deformation velocities [V_S (black solid line) and V_L (red dotted line)] versus α computed using $v_0 = 1$, $\sigma_S = 0.5$, $\sigma_L = 1$ and $\tau = 2.5$ up to 15.

et al. (2007), Davydov (1991), Scott (1992). In our work, we will use $J = 0.1$, which is in alignment with previous research Hennig et al. (2007), Davydov (1991), Scott (1992), Korotin et al. (2015), Satija et al. (1980), Hutchings et al. (1979), Kadota et al. (1967). The value of τ will be adjustable, but in previous works, it was typically chosen to be around 10 Hennig et al. (2007), Ranciaro-Neto & de Moura (2016), Sales et al. (2018) due to potential differences in time scales between quantum and classical propagation. However, we will explore the effects of varying τ around this value. Our initial conditions will be $u_y(t = 0) = Ae^{-(y-N/2)^2/(4\sigma_S^2)}$, $X_y(t = 0) = 0$, and $P_y(t = 0) = e^{-(y-N/2)^2/(4\sigma_L^2)}$, with A as a normalization constant. We will use a Taylor procedure de Moura (2011) to solve the set of equations 3, and a standard second-order Verlet's like procedure Allen & Tildesley (1987), da Silva et al. (2019) to solve the lattice dynamics. Our analysis will focus on magnon propagation and lattice deformation dynamics along the chain, which can be observed using the quantity n_S defined as Sales et al. (2018):

$$n_S = \sum_y (y - N/2) |u_y(t)|^2. \tag{5}$$

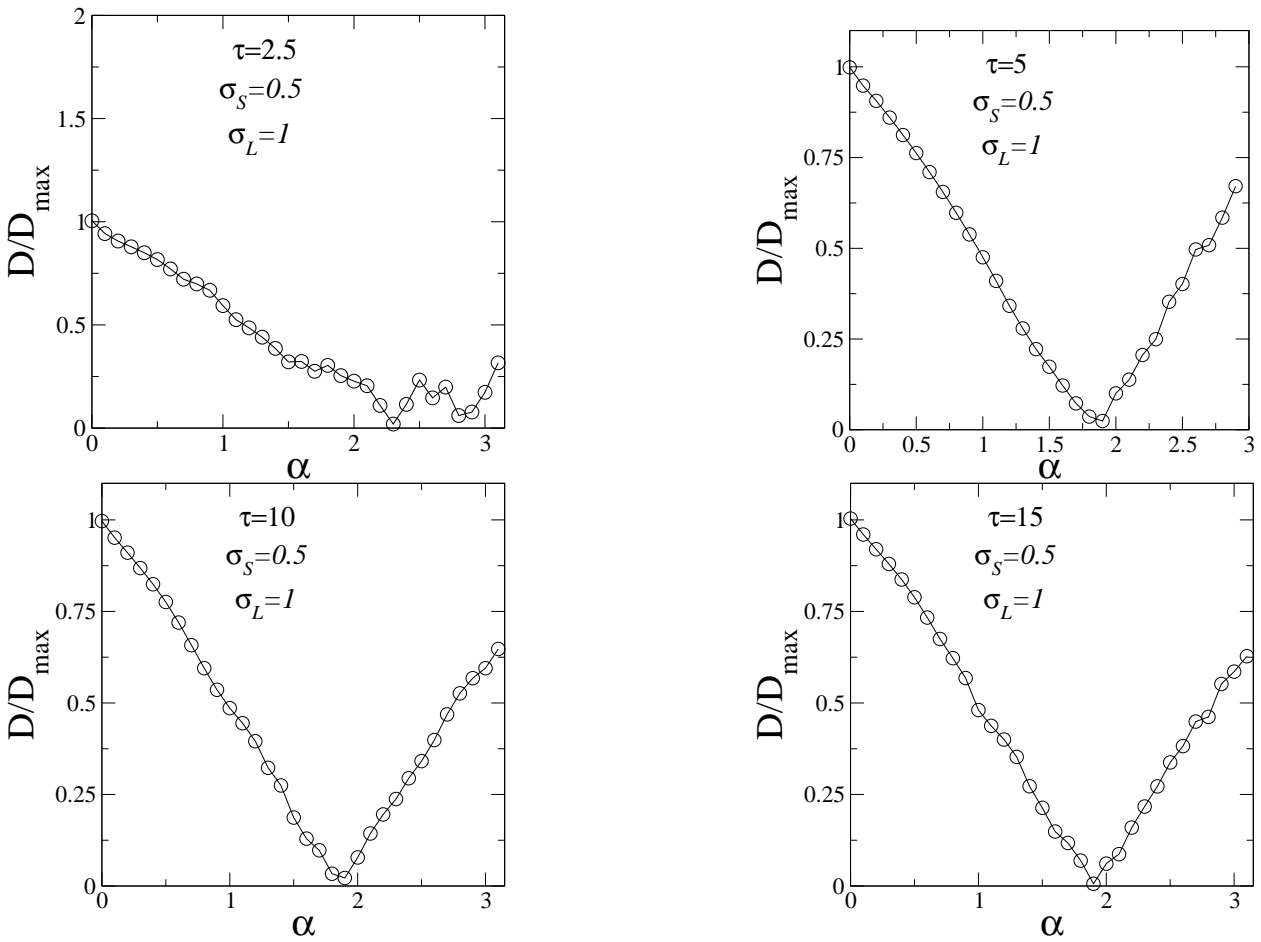


Figure 6. The normalized distance between the Magnon and the lattice deformation (D/D_{max}) versus α computed for $v_0 = 1$, $\sigma_s = 0.5$, $\sigma_L = 1$ and $\tau = 2.5$ up to 15.

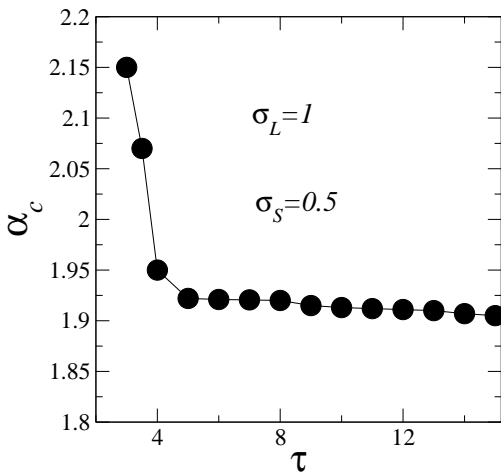


Figure 7. The critical value α_c versus τ for $\sigma_s = 0.5$ and $\sigma_L = 1$.

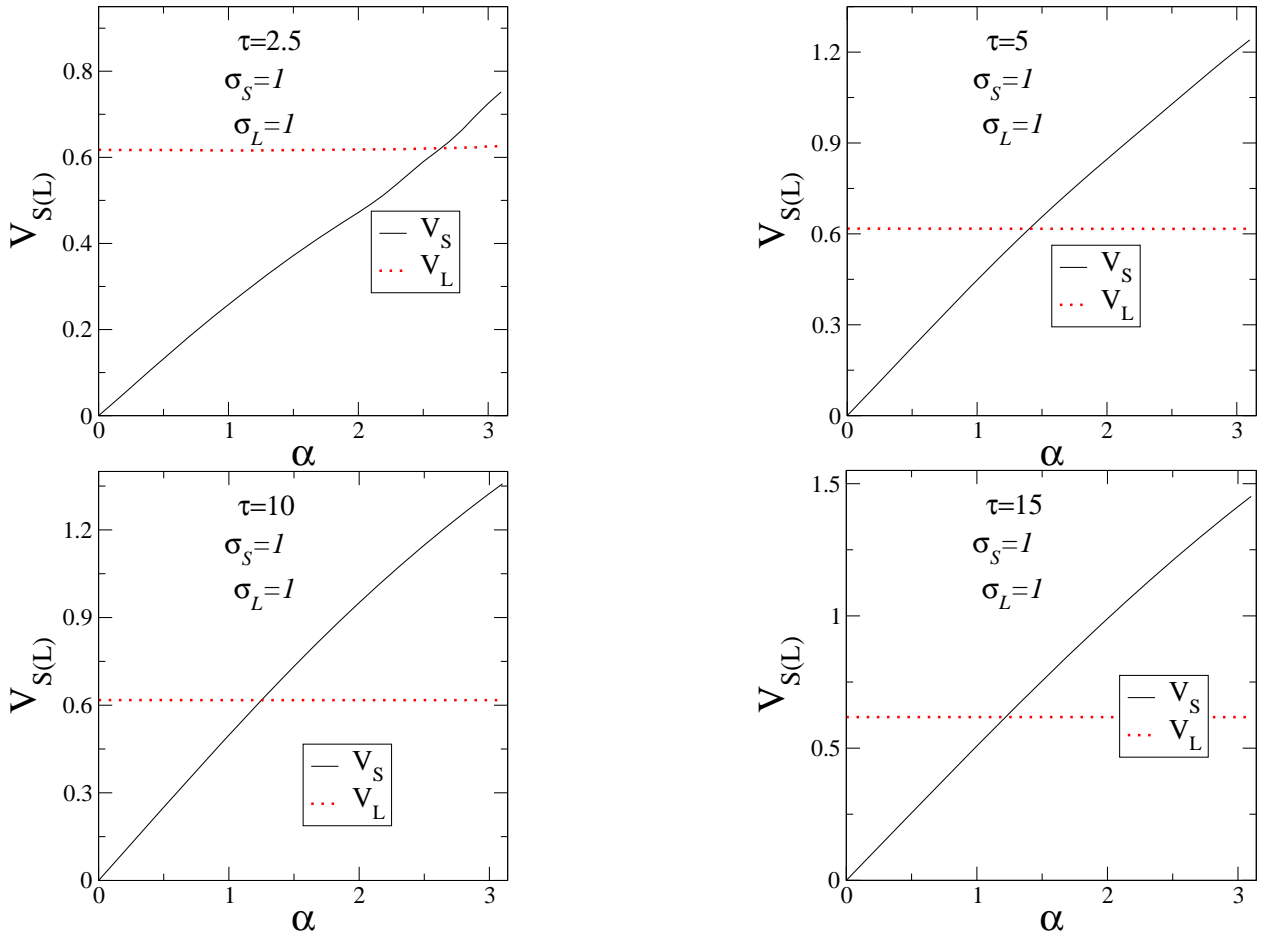


Figure 8. The velocities [V_S (black solid line) and V_L (red dotted line)] versus α computed using $v_0 = 1$, $\sigma_S = 1$, $\sigma_L = 1$ and $\tau = 2.5$ up to 15.

The lattice properties can be analyzed using the mean position of the lattice deformation defined as:

$$n_L = \frac{\sum_y (y - N/2) [1 - e^{-(x_y - x_{y-1})}]^2}{\sum_y [1 - e^{-(x_y - x_{y-1})}]^2}. \tag{6}$$

We want to emphasize that n_S and n_L represent the mean position of the spin-wave excitation and the lattice deformation, respectively. These measurements generally are in units of lattice spacing ($l_s = 1$). Using these quantities, we can obtain the magnon and the lattice deformation velocities V_S and V_L using fittings of the curves $n_S \times t$ and $n_L \times t$. We stress that here we will use a methodology similar to that was used in the previous literature Hennig et al. (2007), Sales et al. (2018). We will follow the propagation of the magnon and the lattice deformation to describe the existence (or not) of magnon-lattice coupled movement. Generally, stable dynamics with $n_S \approx n_L$ and $V_S \approx V_L$ indicate the presence of magnon-lattice pair formation. The nonlinear Morse chain considered here contains a solitonic mode propagation along the chain. We can see this solitonic mode by calculating the lattice deformation Z_y ; this quantity represents a generalized probability that deformation around site y occurs. This is obtained by normalizing $B_y = (1 - e^{[-x_y + x_{y-1}]}]^2$, that is $Z_y = B_y / \sum_y (B_y)$. We will plot

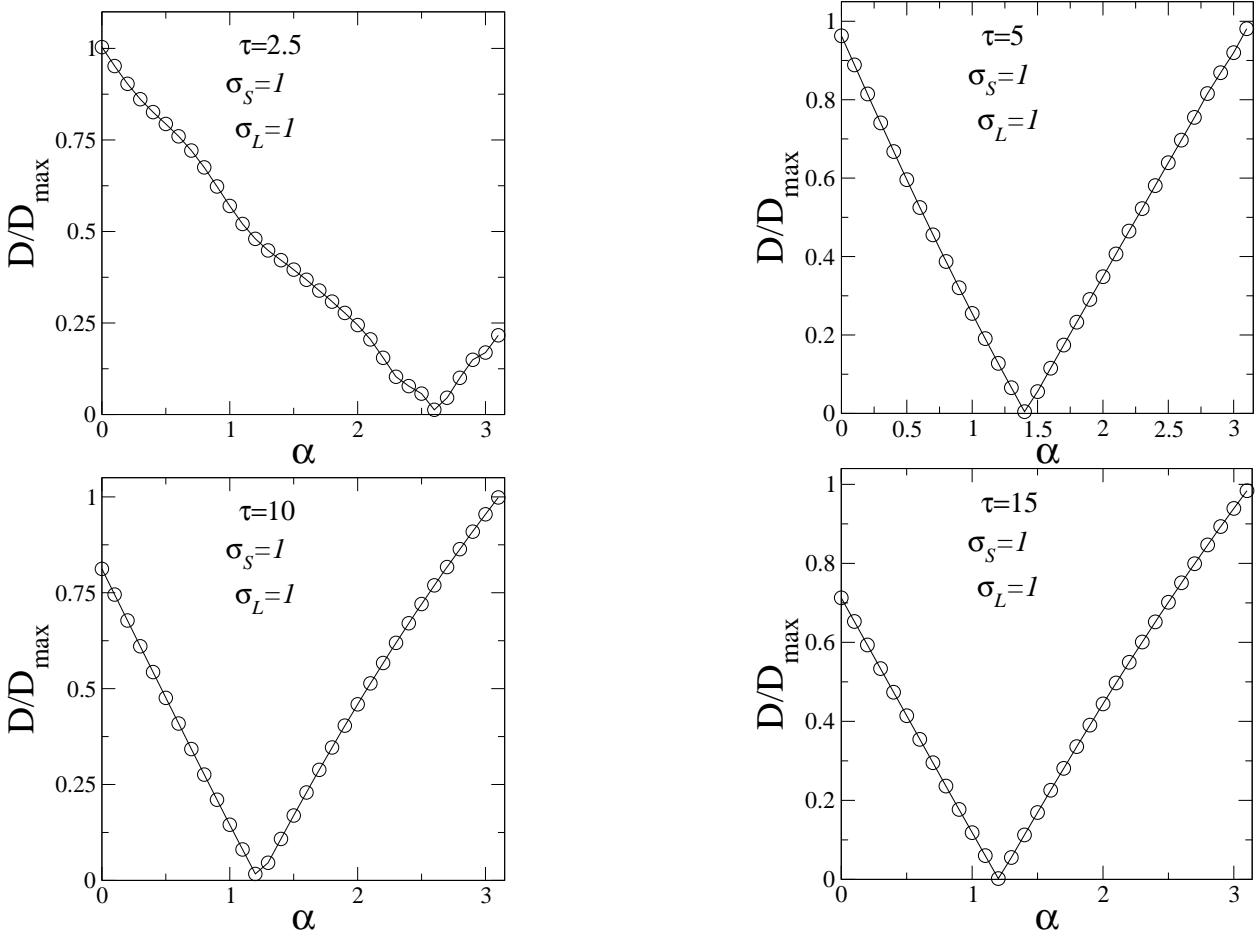


Figure 9. The normalized distance between the Magnon and the lattice deformation (D/D_{max}) versus α computed for $v_0 = 1$, $\sigma_s = 1$, $\sigma_L = 1$ and $\tau = 2.5$ up to 15.

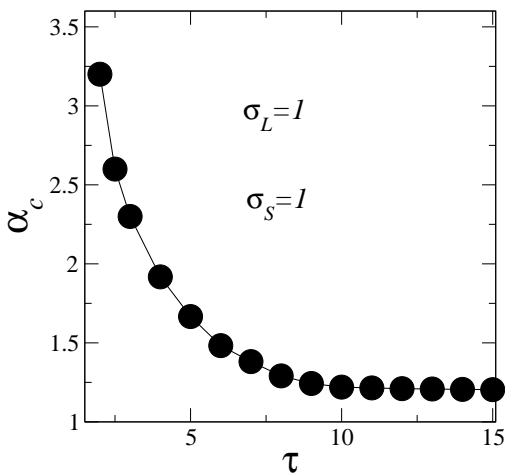


Figure 10. The critical value α_c versus τ for $\sigma_s = \sigma_L = 1$.

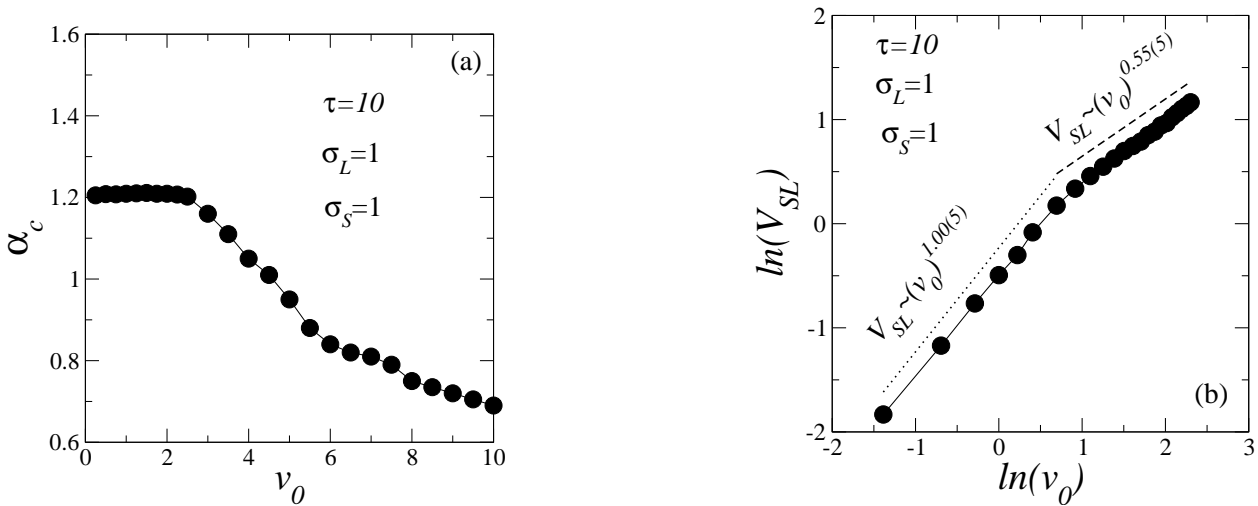


Figure 11. a) The critical value α_c versus v_0 ; b) The magnon-soliton velocity V_{SL} versus v_0 . Calculations were done for $\sigma_L = \sigma_S = 1$ and $\tau = 10$.

$Z_n \times t \times n$ where $n = y - N/2$ (i.e., $n = 0$ represents the center of the chain). In fig. 1 we plot our results for $\alpha = 0, 1, 2, 3$, $v_0 = 1$, $\sigma_S = 0.5$, $\sigma_L = 0.5$ and $\tau = 10$. We can see that independent of the value of α , the lattice deformation exhibits a stable solitonic mode propagating along the chain. Therefore, the main focus of our work is investigating the existence of a possible magnon-soliton pair formation and its dependence on all tunable parameters.

RESULTS AND DISCUSSION

Our findings on the velocities V_S and V_L in relation to α are presented below. We obtained V_S and V_L through the linear fitting of the curves $n_S \times t$ and $n_L \times t$. Our calculations of n_S and n_L suggest that both quantities exhibit long-term linear behavior, consistent with the solitonic dynamics found in references Sales et al. (2018). We performed these calculations using a time limit of $t_{max} \approx 10^4$. The linear fitting was conducted using the last 20% of the complete time interval, roughly within the time interval [8000, 10000]. We used a Taylor expansion up to the tenth order to solve the quantum equations and a second-order Verlet-like method to solve the classical equations. We performed our numerical procedure using a time step of $\Delta t = 0.001$. It is important to emphasize that this method is faster than the Runge-Kutta formalism de Moura & Domínguez-Adame (2008) for this type of problem. The initial condition was given by : $u_y(t = 0) = A e^{-(y-N/2)^2/(4\sigma_S^2)}$, $X_y(t = 0) = 0$ and $P_y(t = 0) = v_0 e^{-(y-N/2)^2/(4\sigma_L^2)}$. Here, A is a normalization constant, v_0 is a tunable parameter, and the σ_L and σ_S are larger than zero. We varied the parameter τ within the interval [1, 15]. We considering initially $v_0 = 1$, $\sigma_S = 0.5$, $\sigma_L = 0.5$ and several values of τ . We show our results in figs. 2(a-d). We emphasize that the curves indicate the velocities V_S (black solid line) and V_L (red dotted line) versus α for several values of τ . To construct these curves, we calculate the dynamics of the spin and the lattice for long times for several values of α and τ . We calculate the V_S and V_L curves versus α using a linear fitting. We can see that V_L is roughly independent of α . On another side, spin propagation strongly depends on the spin-lattice interaction parameter α . Let us clarify this important matter in simpler

terms. The lattice's deformation is governed by eq. 4. We can see that when α is small, the nonlinear Morse terms, i.e., the first two terms, dominate over the terms that depend directly on α and the wave functions. Therefore, the soliton velocity remains roughly constant; however, when α increases, the final terms become more significant and have a greater impact on the soliton propagation, causing a slight increase in velocity. On a different note, the behavior of spin dynamics is dictated by equation 3, which shows a significant dependence on the magnitude of α in both the diagonal (first term) and the off-diagonal (last two terms). As such, it was indeed expected that the value of α would influence the magnon's velocity. By analyzing all curves for several of τ we have considered, there is a matching of the magnon's and lattice's velocity ($V_S \approx V_L$) for a specific value of α . This result suggests that for this particular value of α , the magnon and the lattice deformation travel at the same velocity. We stress that it is the first indication that magnon and lattice may move in a kind of "correlated propagation" (like a magnon-lattice pair formation). We can also see that as the parameter τ has increased, this value of α in which the velocities are the same become smaller. To comprehend this phenomenon, we need to emphasize that when τ increases, the off-diagonal terms in the Schrödinger equation become more effective. This results in a stronger coupling with the lattice deformation even for smaller values of α .

We also calculate the long-time mean distance between the magnon and the lattice deformation. The distance is defined as $D = |n_L(t \rightarrow \infty) - n_S(t \rightarrow \infty)|$. We emphasize that D represents also an measurement of the possible existence of the magnon-soliton pair state. In general, bound states exhibit a smaller value of intrinsic internal distances. Dias et al. (2007) used this kind of measure to detect the existence of electron-electron bound states in the low-dimensional two-electron Hubbard model. We emphasize that we will plot (see figs. 3(a-d)) D/D_{max} versus α where D_{max} represents the maximum of the distance between the magnon and the lattice position. We can observe that for the same value of α in which that $V_L \approx V_S$, we can see that $D/D_{max} \approx 0$, i.e., the magnon and the lattice position are close, thus suggesting the existence of magnon-lattice pair formation. We can see that the critical value of α in which $D/D_{max} \approx 0$ is in good agreement with the critical value found using the velocity curves versus α (see fig. 2). Therefore all measures of D/D_{max} , V_S , and V_L are topological quantities that characterize the propagation of the magnon and the lattice deformation. Our calculations numerically demonstrate that for some specific values of $\alpha = \alpha_c$, the distance D is small, and the magnon and the lattice deformation travel at the same velocity. This result strongly indicates a magnon-soliton pair formation for these special situations.

In fig. 4, we collect the critical value of α versus τ . We stress that for $\alpha = \alpha_c$ the system exhibits a magnon-lattice pair formation, i.e., the magnetic excitation moves along with the lattice vibration and at the same velocity. We emphasize again that the decreasing of α_c with τ is a direct consequence of the role played by τ at the off-diagonal terms at eq. 3. As the τ is increased, the effective off-diagonal term also increases. Increasing the effective spin-spin interaction makes coupling between the spin and the lattice deformations easier. In figures 5 and 6 we consider again $v_0 = 1$ and change the values of σ_S and σ_L respectively to 0.5 and 1; we kept the same range of values of τ . We can observe that the results are qualitatively the same obtained in figs. 2 and 3 i.e.: as the value of τ is increased, the magnon-lattice pair formation is obtained for a specific value of $\alpha = \alpha_c$. We also obtained that as τ is increased α_c decreases (see fig. 7). In figures 8 and 9, we show our results considering $\sigma_S = 1$ and $\sigma_L = 1$, and we kept the same range of values of τ and v_0 . The results obtained are similar to those

in the previous figures. It appears that the magnon-lattice pair only exists when α equals the critical value α_c . This critical value decreases as τ increases, as shown in figure 10.

To summarize the previous results, an initial vibrational Gaussian velocity pulse was introduced into the lattice, and a finite amount of the initial energy propagated along the lattice through the nonlinear solitonic mode. This behavior was observed by tracking the lattice position over time, with our calculations indicating that a finite fraction of the initial energy remained trapped in a finite region of the lattice. This localized pulse could travel along the lattice with a constant velocity of V_L . Additionally, the quantum equation was initialized using a Gaussian initial magnon wave packet, and our calculations showed that the dominant wave packet exhibited a solitonic profile with a position given by $n_S(t) \approx V_S t$. By computing V_S and V_L , we numerically demonstrated that depending on the value of magnon-lattice coupling, we could obtain a good indication of magnon-soliton pair formation. For certain values of $\alpha = \alpha_c$, our calculations indicated that $n_S \approx n_L$ and $V_S \approx V_L$. In ref. Sales et al. (2018), the possibility of magnon-soliton propagation in nonlinear lattices was demonstrated considering localized initial states (i.e., $\sigma_L = \sigma_S = 0$). However, we have discovered that broad initial conditions can also lead to magnon-soliton propagation. The critical value for the occurrence of magnon-solitons depends on the width of the initial conditions and the value of τ . The parameter τ measures the time scale difference between the magnon and lattice deformation and acts as the intensity of the effective spin-spin interaction within the quantum equations. This spin-spin interaction is also the key to the magnon-lattice interaction. As τ increases, the spin-lattice terms become stronger, making it easier to promote magnon-soliton pair formation.

Before we finish our work, we need to examine how our results vary with the value of v_0 . Specifically, we want to see how the formation of magnon-soliton pairs is affected by the strength of the initial impulse. To do this, we conducted many numerical experiments with different values of v_0 , which allowed us to observe the signatures of magnon-soliton pairs. We discovered that within the range of v_0 values between 1 and 10, a magnon-soliton pair exists when α equals a certain value, denoted as α_c . However, this critical value depends on the value of v_0 . For instance, the results we obtained for $\sigma_S = \sigma_L = 1$ and $\tau = 10$ (refer to fig. 11(a)) revealed that when v_0 is low (less than 3), the critical value remains stable at around $\alpha_c = 1.205$, while for v_0 values greater than 3, the critical value decreases by approximately half. This decrease in α_c with increasing v_0 may seem counterintuitive, but we believe it is mainly due to the intensity of the solitonic mode. As the initial impulse grows, the soliton gains more intensity, resulting in an increased spin-lattice interaction that favors the magnon-soliton pairing. Our calculations show that regardless of the values of σ_L and σ_S , the results remain qualitatively the same. The velocity of the magnon-soliton pair (V_{SL}) is also dependent on the initial velocity v_0 . In fig. 11(b), we observe that for small v_0 , $V_{SL} \propto v_0$. For $v_0 > 3$, $V_{SL} \propto v_0^{0.55(5)}$. It is essential to note that the results shown in fig. 11 do not depend on the values of σ_L , σ_S , and τ . Generally, as velocity increases, the solitonic mode becomes faster, resulting in a faster magnon-soliton pair.

SUMMARY AND CONCLUSIONS

Our research delves into the behavior of a single magnon state in a nonlinear Morse chain, considering the magnon-lattice coupling through the Heisenberg spin-spin term that directly depends on the spin positions. We begin with a Gaussian wave packet for the magnon state and a Gaussian impulse

packet for the lattice. The velocity intensity and width of these initial Gaussian pulses are adjustable parameters in our model. We also vary the time scales between the magnon and lattice dynamics. We provide a detailed numerical analysis of how magnon-soliton pairs propagate and their dependence on these parameters. Our findings reveal that magnon-soliton propagations are attainable for specific values of the magnon-lattice interaction (called α_c in our model) and that this critical value is highly reliant on the width of the initial Gaussian pulses. Our numerical calculations indicate that increasing the velocity of the initial Gaussian pulse decreases the critical value of spin-lattice interaction (α_c). Furthermore, as the time difference between the magnon and lattice dynamics increases, the intensity of magnon-lattice coupling needed to promote pair formations decreases. Overall, our study underscores the importance of the initial conditions and the specifics of the magnon/lattice dynamics in the existence of magnon-soliton pairs in nonlinear chains. We demonstrate that a time difference of $\tau \geq 10$ yields a more reliable existence of magnon-lattice coupling, consistent with previous research. Our work is intended to inspire further research in this area.

Acknowledgments

This work was partially supported by Conselho Nacional de Desenvolvimento Científico e Tecnológico (CNPq), Coordenação de Aperfeiçoamento de Pessoal de Nível Superior (CAPES) and Financiadora de Estudos e Projetos (FINEP), CNPq-Rede Nanobioestruturas, as well as FAPEAL (Alagoas State Agency).

REFERENCES

- ALLEN MP & TILDESLEY TJ 1987. Computer Simulation of Liquids. Oxford University Press, p. 71-80.
- CARRILLO JA, MARTIN S & PANFEROV V 2013. A new interaction potential for swarming models. *Physica D: Nonlinear Phenomena* 260: 112-126.
- CHALLALI R, SAIT S, BOURAHLA B & FERRAH L 2023. Localized Surface Magnon Modes in Cubic Ferromagnetic Lattices. *SPIN* 13: 2350001.
- CHEN C, LI Y & ZHANG J 2023. Characteristics of magnon-phonon coupling in magnetic insulator based on the Boltzmann equation. *AIP Advances* 13: 025221.
- CONG A, LIU J, XUE W, LIU H, LIU Y & SHEN K 2022. Exchange-mediated magnon-phonon scattering in monolayer CrI_3 . *Phys Rev B* 106: 214424.
- EVANGELOU SN & KATSANOS DE 1992. Super-diffusion in random chains with correlated disorder. *Phys Lett A* 164: 456-464.
- DA SILVA LD, RANCIARO-NETO A, SALES MO, DOS SANTOS JLL & DE MOURA FABF 2019. Propagation of vibrational modes in classical harmonic lattice with correlated disorder. *Ann Braz Acad Sci* 91(2): e20180114.
- DAVYDOV AS 1991. Solitons in Molecular Systems. 2nd ed., Reidel, Dordrecht.
- DE LIMA EF & DE CARVALHO RE 2012. Effects of oscillatory behavior of the dipole function on the dissociation dynamics of the classical driven Morse oscillator. *Physica D: Nonlinear Phenomena* 241: 1753-1757.
- DE MOURA FABF, COUTINHO-FILHO MD, RAPOSO EP & LYRA ML 2002. Delocalization and spin-wave dynamics in ferromagnetic chains with long-range correlated random exchange. *Phys Rev B* 66: 014418.
- DE MOURA FABF 2011. Dynamics of one-electron in a one-dimensional systems with an aperiodic hopping distribution. *Int J M Phys C* 22: 63-69.
- DE MOURA FABF & DOMÍNGUEZ-ADAME F. 2008. Extended modes and energy dynamics in two-dimensional lattices with correlated disorder. *Eur Phys J B* 66: 165-169.
- DIAS WS, NASCIMENTO EM, LYRA ML & DE MOURA FABF 2007. Frequency doubling of Bloch oscillations for interacting electrons in a static electric field. *Phys Rev B* 76: 155124.
- GRIES L, JONAK M, ELGHANDOUR A, DEY K & KLINGELER R 2022. Role of magnetoelastic coupling and magnetic anisotropy in MnTiO_3 . *Phys Rev B* 106: 174425.
- HAYASHI H & ANDO K 2018. Spin Pumping Driven by Magnon Polarons. *Phys Rev Lett* 121: 237202.
- HENNIG D, CHETVERIKOV A, VELARDE MG & EBELING W 2007. Electron capture and transport mediated by lattice solitons. *Phys Rev E* 76: 046602.

- HOLANDA J, MAIOR DS & AZEVEDO A 2018. Detecting the phonon spin in magnon-Phonon conversion experiments. *Nature Phys* 14: 500-506.
- HUTCHINGS MT, MILNE JM & IKEDA H 1979. Spin wave energy dispersion in $KCuF_3$: a nearly one-dimensional spin-1/2 antiferromagnet. *Journal of Physics C: Solid State Physics* 12: L739.
- IKEDA K, DOI Y, FENG BF & KAWAHARA T 2007. Chaotic breathers of two types in a two-dimensional Morse lattice with an on-site harmonic potential. *Physica D: Nonlinear Phenomena* 225: 184-196.
- KADOTA S, YAMADA I, YONEYAMA S & HIRAKAWA K 1967. Formation of One-Dimensional Antiferromagnet in $KCuF_3$ with the Perovskite Structure. *Journal of the Physical Society of Japan* 23: 751-756.
- KOROTIN DMM, MAZURENKO VV, ANISIMOV VI & STRELTSOV SV 2015. Calculation of exchange constants of the Heisenberg model in plane-wave-based methods using the Green's function approach. *Phys Rev B* 91: 224405.
- LI J, SIMENSEN HT, REITZ D, SUN Q, YUAN W, LI C, TSEKOVNYAK Y, BRATAAS A & SHI J. 2020. Observation of Magnon Polarons in a Uniaxial Antiferromagnetic Insulator. *Phys Rev Lett* 125: 217201.
- LI Y, ZHAO C, ZHANG W, HOFFMANN A & NOVOSAD V. 2021. Advances in coherent coupling between magnons and acoustic phonons. *APL Materials* 9: 060902.
- LUO J ET AL. 2023. Evidence for Topological Magnon-Phonon Hybridization in a 2D Antiferromagnet down to the Monolayer Limit. *Nano Lett* 23: 2023-2030.
- MASCIOCCHI G ET AL. 2022. Control of magnetoelastic coupling in Ni/Fe multilayers using He^+ ion irradiation. *Appl Phys Lett* 121: 182401.
- MINGRAN X, KEI Y, JORGE P, KORBINIAN B, BIVAS R, KATSUYA M, HIROMASA T, DIRK G, SADAMICHI M & YOSHICHIKA O. 2020. Nonreciprocal surface acoustic wave propagation via magneto-rotation coupling. *Science Advances* 6: 32.
- MORAIS D, LYRA ML, DE MOURA FABF & DIAS WS. 2020. The self-trapping transition of one-magnon excitations coupled to acoustic phonons. *Journal of Magnetism and Magnetic Materials* 506: 166798.
- MORAIS D, DE MOURA FABF & DIAS WS. 2021. Magnon-polaron formation in XXZ quantum Heisenberg chains. *Phys Rev B* 103: 195445.
- RANCIARO-NETO A & DE MOURA FABF. 2016. Electronic dynamics under effect of a nonlinear Morse interaction and a static electric field. *Commun Nonlinear Sci Numer Simulat* 40: 6-14.
- SALES MO, NETO AR & DE MOURA FABF. 2018. Spin-wave dynamics in nonlinear chains with spin-lattice interactions. *Phys Rev E* 98: 062136.
- SALES MO, NETO AR & DE MOURA FABF. 2023. Magnon-lattice dynamics in a Heisenberg-Morse model with spin-lattice interaction. *Physica D: Nonlinear Phenomena* 443: 133564.
- SASAKI R, NII Y & ONOSE Y. 2021. Magnetization control by angular momentum transfer from surface acoustic wave to ferromagnetic spin moments. *Nat Commun* 12: 2599.
- SATIJA SK, AXE JD, SHIRANE G, YOSHIKAWA H & HIRAKAWA K. 1980. Neutron scattering study of spin waves in one-dimensional antiferromagnet $KCuF_3$. *Phys Rev B* 21: 2001.
- SCOTT AC. 1992. Davydov's soliton. *Phys Rep* 217: 1-67.
- SUN Y-J, LAI J-M, PANG S-M, LIU X-L, TAN P-H & ZHANG J 2022. Magneto-Raman Study of Magnon-Phonon Coupling in Two-Dimensional Ising Antiferromagnetic $FePS_3$. *Phys Chem Lett* 13: 1533-1539.
- WEILER M, HUEBL H, GOERG FS, CZESCHKA FD, GROSS R & GOENNENWEIN STB. 2012. Spin Pumping with Coherent Elastic Waves. *Phys Rev Lett* 108: 176601.
- XIONG Z, DATTA T, STIWINTER K & YAO D-X 2017. Magnon-phonon coupling effects on the indirect K-edge resonant inelastic x-ray scattering spectrum of a two-dimensional Heisenberg antiferromagnet. *Phys Rev B* 96: 144436.
- ZHANG X, ZHANG Y, OKAMOTO S & XIAO D. 2019. Thermal Hall Effect Induced by Magnon-Phonon Interactions. *Phys Rev Lett* 123: 167202;
- ZHANG S, GO G, LEE K-J & KIM SK. 2020. $SU(3)$ Topology of Magnon-Phonon Hybridization in 2D Antiferromagnets. *Phys Rev Lett* 124: 147204.

How to cite

SANTOS JUNIOR MS, SALES MO & DE MOURA FABF. 2023. Magnon-lattice propagation in a Morse chain: the role played by the spin-lattice interaction and the initial condition. *An Acad Bras Cienc* 95: e20230408. DOI 10.1590/0001-3765202320230408.

Manuscript received on April 12, 2023;
accepted for publication on August 31, 2023

MARCONI SILVA SANTOS JUNIOR¹
<https://orcid.org/0009-0001-1932-6559>

MESSIAS DE OLIVEIRA SALES²
<https://orcid.org/0000-0001-5116-0301>

FRANCISCO ANACLETO BARROS FIDELIS DE MOURA¹
<https://orcid.org/0000-0002-4446-0450>

¹Universidade Federal de Alagoas, Instituto de Física, Av. Lourival Melo Mota, s/n, Tabuleiro do Martins, 57072-900 Maceió, AL, Brazil

²Instituto Federal do Maranhão, Campus São João dos Patos, Rua Padre Santiago, s/n, Centro, 65665-000 São João dos Patos, MA, Brazil

Correspondence to: **Francisco Anacleto Barros Fidelis de Moura**

E-mail: fidelis@fis.ufal.br

Author contributions

M.S.S. Junior and F. A. B. F. de Moura did all calculations of the figures; M.O. Sales and F. A. B. F. de Moura written the manuscript.

